

COMMUNICATION

[View Article Online](#)
[View Journal](#) | [View Issue](#)

Cite this: *Dalton Trans.*, 2025, **54**, 12760

Received 19th June 2025,
Accepted 23rd July 2025

DOI: 10.1039/d5dt01440a

rsc.li/dalton

Direct covalent immobilization of the Hoveyda–Grubbs catalyst without molecular modification for achieving economical and efficient olefin metathesis†

Chuangchuang He, Jincheng Duan, Yang Zhou, Junling Cui and Xuebing Ma *

The direct covalent immobilization of the Hoveyda–Grubbs catalyst into hollow mesoporous polystyrene nanospheres is developed via Friedel–Crafts alkylation without molecular modification for economical and efficient olefin metathesis.

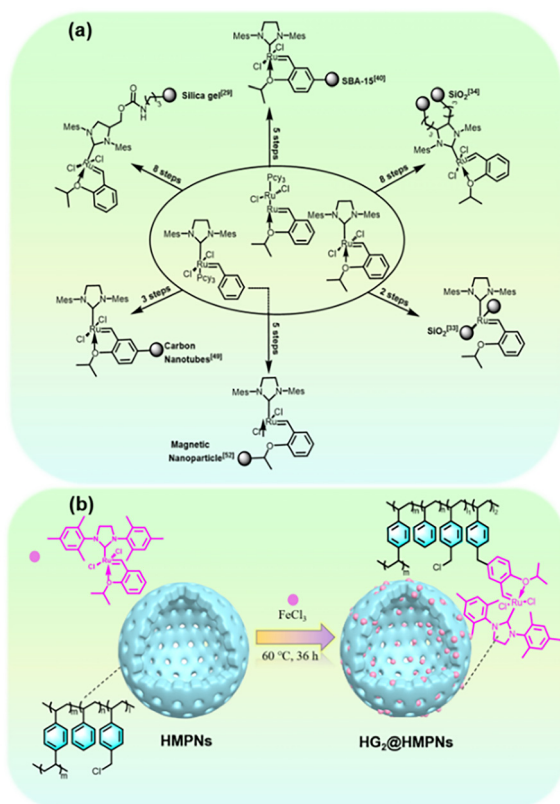
Olefin metathesis reactions including ring-closing, cross-metathesis, acyclic diene polymerization, and ring-opening polymerization, catalysed by 1st and 2nd generation Hoveyda–Grubbs (HG) catalysts, are effective and powerful tools for the construction of carbon–carbon bonds,¹ with broad applications in the synthesis of valuable pharmaceuticals,² fine chemicals,³ advanced polymers,⁴ and in the transformation of biomass into value-added chemicals.⁵ Although homogeneous olefin metathesis offers obvious advantages in catalytic activity, the high cost of HG catalysts and their limited recoverability and reusability from reaction mixtures severely hinder their industrial-scale application. Currently, three main strategies have been developed to achieve the recovery and reuse of HG catalysts, involving encapsulation of HG catalysts in confined spaces,^{6–10} homogeneous catalysis/two-phase separation,¹¹ and immobilization of HG catalysts onto solid supports.¹² The encapsulation of HG catalysts into confined spaces enables the catalysts to promote reactions in a homogeneous-like manner, requiring no molecular modification. Unfortunately, precise control over the pore sizes of the confined spaces is extremely difficult and leads to loss of the HG catalyst. With respect to the unique advantages of homogeneous catalysis, several catalytic and two-phase separation systems, including tagged switchable-phase catalysts,¹³ soluble polymer-supported catalysts,¹⁴ light-controlled and pH-controlled phase strategies,^{15,16} fluorinated catalysts,¹⁷ and nanofiltration,¹⁸ have been developed to achieve homogeneous reactions in one phase followed by separation of HG catalysts in

another phase. However, to meet the demands of homogeneous catalysis, HG catalysts require multi-step molecular modifications. The immobilization of homogeneous HG catalysts onto solid supports, which not only facilitates their separation from the reaction mixture but also realizes catalyst recycling, has become a promising strategy in both academic research and industrial applications. To date, many solid supports, such as silica-based,^{19–40} polymer-based,^{41–46} carbon-based,^{47–50} and magnetic particle-based^{51–53} materials, have been developed to achieve the recovery and reuse of catalysts after the completion of catalytic reactions. Nevertheless, time- and energy-consuming multi-step molecular modifications of HG catalysts are also required to install anchoring groups, such as silanization agents,^{33–36} 3-pyridyl bromide,^{30,43} amides,³⁷ hydroxylates⁴⁶ and exchangeable ligands,^{22,26,44} which enable HG catalysts to easily react with solid supports to achieve their effective immobilization (Scheme 1a). Therefore, it is highly desirable to develop a simple, convenient and general strategy for anchoring expensive HG catalysts onto catalyst supports to realize low-cost chemical synthesis.

Inspired by the direct immobilization of expensive metal complexes and chiral organocatalysts onto catalyst supports without molecular modification *via* Suzuki coupling,⁵⁴ Scholl reaction,⁵⁵ and Friedel–Crafts alkylation,^{56–60} the present study applies Friedel–Crafts alkylation to immobilize the HG catalyst, (1,3-bis(2,4,6-trimethylphenyl)-2-imidazolidinylidene) dichloro(*o*-isopropylphenylmethylene) ruthenium (HG₂), directly onto hollow mesoporous polystyrene nanospheres (HMPNs) to fabricate an HMPN-supported catalyst (HG₂@HMPNs) (Scheme 1b). Compared with previously reported multi-step immobilization strategies (Scheme 1a), this direct immobilization avoids multi-step molecular modification and effectively improves the utilization of the expensive HG₂ catalyst. In particular, the as-prepared HG₂@HMPNs possess a well-defined morphology with thin mesoporous shell and hollow interior, providing an ideal architectural structure for the reactants to rapidly access Ru catalytic sites. In the heterogeneous olefin metathesis of allylbenzoates and croto-

College of Chemistry and Chemical Engineering, Southwest University, Chongqing 400715, PR China. E-mail: zcj123@swu.edu.cn

† Electronic supplementary information (ESI) available. See DOI: <https://doi.org/10.1039/d5dt01440a>



Scheme 1 (a) Synthetic routes for the covalent immobilization of expensive HG catalysts onto solid supports: multi-step molecular modification reported in previous works. (b) Direct covalent immobilization of HG₂ catalyst onto HMPNs described in the present work (b).

naldehyde, HG₂@HMPNs exhibit comparable catalytic yields to the homogeneous HG₂ catalyst.

Owing to the electron-rich 2-isopropoxyphenyl moiety in the molecular structure of the HG₂ catalyst, the Friedel–Crafts alkylation occurs between HMPN-attached benzyl chloride (–C₆H₄CH₂Cl) and 2-isopropoxyphenyl in the HG₂ catalyst. The conditions of the Friedel–Crafts alkylation including temperature, reaction time and the amount of FeCl₃ used are screened and the loading capacities of the HG₂ catalyst are shown in Table S1.† Under the optimal reaction conditions (60 °C, 36 h, 20 mol% FeCl₃), the highest loading capacity of HG₂ catalyst in HG₂@HMPNs is determined by ICP-OES to be 0.46 mmol g^{−1}.

The successful immobilization of the HG₂ catalyst onto the porous shell of HMPNs is confirmed by FT-IR, solid-state ¹³C CP/MAS NMR and XPS spectra (Fig. 1). Compared with pristine HMPNs and free HG₂ catalyst, HG₂@HMPNs exhibits FT-IR characteristic absorption signals of the HG₂ catalyst, including the stretching vibrations of Ru=CH at 2976 cm^{−1} and C–O–C at 1251 cm^{−1}, and the bending vibration of *i*-Pr at 1382 cm^{−1} (Fig. 1a). Furthermore, in the ¹³C CP/MAS NMR spectrum of HG₂@HMPNs (Fig. 1b), signals corresponding to the HG₂ catalyst are observed, including Ru=CH at 288.3 ppm, NCHN at 153.8 ppm, phenyl groups in the range of 120–150 ppm, OCH at 77.1 ppm, and methyl and isopropyl carbons centered at

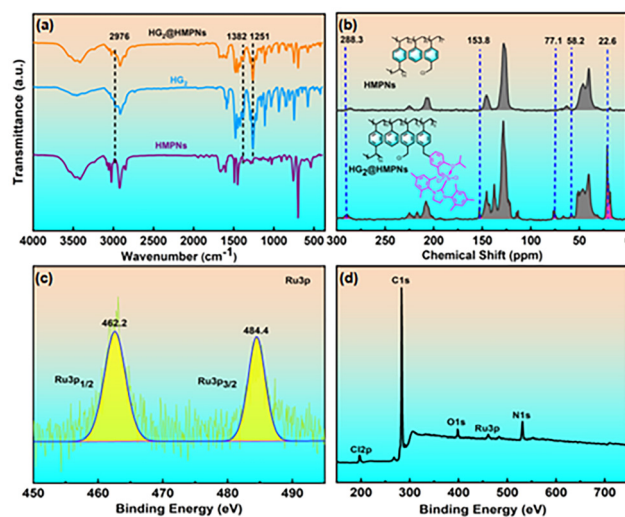


Fig. 1 (a) FT-IR of the HG₂ catalyst, HMPNs and HG₂@HMPNs. (b) Solid-state ¹³C CP/MAS NMR spectra of HMPNs and HG₂@HMPNs. (c) The XPS spectrum of Ru 3p in HG₂@HMPNs and (d) the XPS spectrum of HG₂@HMPNs.

22.6 ppm. The intensity of the chloromethyl signal at 65.1 ppm is weakened, and a new peak at 58.2 ppm is assigned to a –CH₂– linkage emerges, indicating reaction of –CH₂Cl moieties of HMPNs and the electron-rich 2-isopropoxyphenyl group in the HG₂ catalyst. Additionally, the XPS spectra show the binding energies of all elements in HG₂@HMPNs, including C 1s at 283.2 eV, O 1s at 398.7 eV, N 1s at 531.6 eV (Fig. 1d), Ru 3p_{1/2} at 462.2 eV and Ru 3p_{3/2} at 484.4 eV (Fig. 1c), respectively. The binding energy of Cl 2p at 199.5 eV indicates that some benzyl chloride moieties in HMPNs have not been completely consumed during the immobilization of the HG₂ catalyst (Fig. 1d), which is consistent with the result obtained from ¹³C CP/MAS NMR. Based on the above-mentioned results, it is confirmed that the HG₂ catalyst is successfully anchored onto the porous shell of HMPNs *via* a –CH₂– linkage.

As observed from the SEM images (Fig. 2a and b), HG₂@HMPNs retains the well-defined spherical morphology of their parent HMPNs, with particle size distribution of 224 ± 12 nm (*n* = 100) (Fig. 2i) compared to that of 201 ± 12 nm for HMPNs (*n* = 100) (Fig. 2j). Owing to the pillaring effect of the anchored bulky HG₂ catalyst, the particle size of HG₂@HMPNs is increased by about 23 nm. The TEM (Fig. 2e and f) and HAADF (Fig. 2c and d) images, clearly reveal a hollow interior for both HMPNs and HG₂@HMPNs. Furthermore, TEM-EDS elemental mappings of C and N atoms indicate that the HG₂ catalyst is evenly distributed on the porous shell of HG₂@HMPNs (Fig. 2g and h). Upon anchoring of HG₂ onto HMPNs, the resultant HG₂@HMPNs exhibit no significant change in the volume of adsorbed N₂ (Fig. 2k). However, the pore size becomes narrow due to the space occupied by the anchored HG₂ catalyst, and some smaller mesopores centered at 5.2 nm and 7.5 nm are newly constructed in the shell of

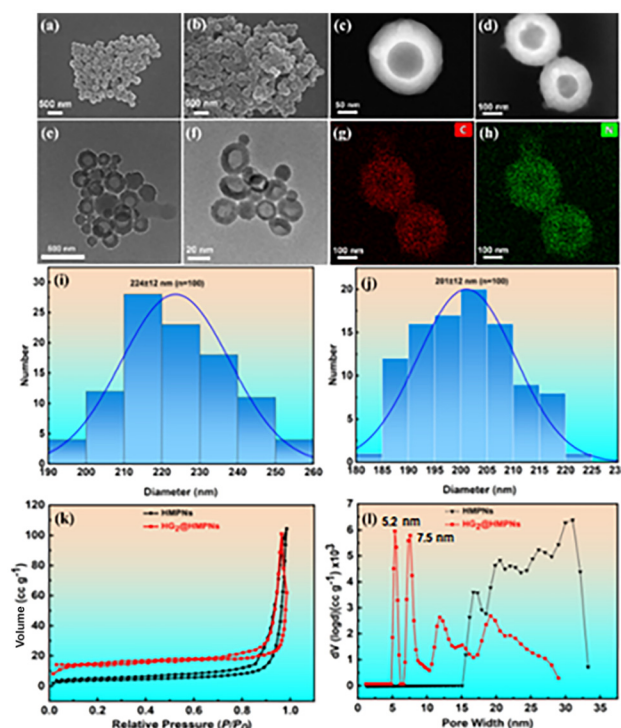


Fig. 2 SEM images of (a) HMPNs and (b) HG₂@HMPNs. HAADF of (c) HMPNs and (d) HG₂@HMPNs. TEM images of (e) HMPNs and (f) HG₂@HMPNs. TEM-EDS mappings of (g) carbon and (h) nitrogen for HG₂@HMPNs. Particle size distributions of (i) HG₂@HMPNs and (j) HMPNs based on the SEM images. (k) N₂ adsorption-desorption isotherms and (l) pore size distributions of HMPNs and HG₂@HMPNs.

HG₂@HMPNs (Fig. 2l). Overall, the as-fabricated HG₂@HMPNs possess spherical morphology similar to their parent HMPNs with a hollow interior and a thin and mesoporous shell, which facilitates fast mass transfer of reactants to the Ru catalytic sites during heterogeneous catalysis.⁶¹

The conditions of the HG₂@HMPN-promoted heterogeneous olefin metathesis reaction between allylbenzoate and crotonaldehyde,⁶² including solvent, reaction temperature and the amount of catalyst used, were optimized and the details are shown in Table 1. When the amount of HG₂ catalyst used in HG₂@HMPNs is set to 1.0 mol%, the product is afforded at its highest yield (39%) in toluene at 20 °C during 30 min of reaction. This result is attributed to non-polar toluene being more suitable than other solvents for the generation of weakly polar intermediates in the catalytic cycle. Upon increasing or decreasing the reaction temperature, no better yield of product is obtained. When the amount of anchored HG₂ catalyst is increased from 1.0 mol% to 5.0 mol%, the yield of product is significantly improved to 83%. However, subsequently doubling the dosage of HG₂ catalyst to 10 mol% leads to a decreased yield (80%), likely due to reduced swellability of HG₂@HMPNs in toluene (2 mL), resulting in narrower pore sizes that restrict access of reactants to the interior Ru catalytic sites.⁵⁷ Furthermore, no better yield is obtained by prolonging the reaction time to 40 min. It is concluded that the best yield

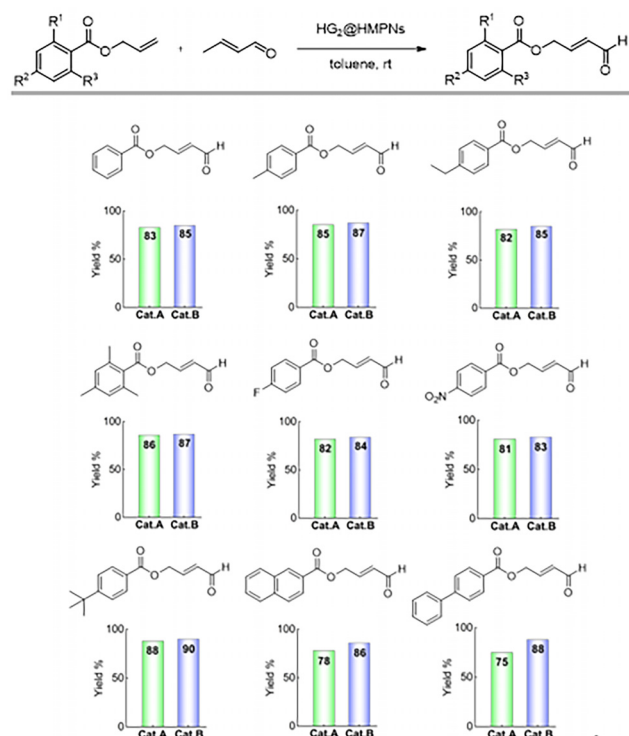
Table 1 Optimization of heterogeneous olefin metathesis reaction conditions^a

Entry	Solvent	Temp. (°C)	Time (min)	Cat. (mol%)	Yield ^b (%)
1	Toluene	20	30	1.0	39
2	DCM	20	30	1.0	28
3	DCE	20	30	1.0	36
4	THF	20	30	1.0	30
5	CHCl ₃	20	30	1.0	33
6	DMF	20	30	1.0	20
7	Acetone	20	30	1.0	25
8	Methanol	20	30	1.0	15
9	Ethanol	20	30	1.0	10
10	DMSO	20	30	1.0	26
11	Toluene	0	30	1.0	21
12	Toluene	30	30	1.0	33
13	Toluene	40	30	1.0	34
14	Toluene	50	30	1.0	32
15	Toluene	60	30	1.0	32
16	Toluene	20	30	3.0	64
17	Toluene	20	30	5.0	83
18	Toluene	20	30	10.0	80
19	Toluene	20	20	5.0	72
20	Toluene	20	40	5.0	83

^a Reaction conditions: allylbenzoate (162.2 mg, 1.0 mmol), crotonaldehyde (70.1 mg, 1.0 mmol), HG₂@HMPNs, solvent (2 mL), 30 min.
^b Isolated yields.

(83%) is obtained during heterogeneous catalysis using HG₂@HMPNs under the following optimal conditions: toluene (2 mL), 5.0 mol% of HG₂ catalyst in HG₂@HMPNs (108.0 mg), substrates (1.0 mmol), 20 °C, 30 min. In particular, the self-metathesis of allylbenzoate has also been confirmed,⁶² while crotonaldehyde is not fully consumed under the optimized conditions.

Under the optimal reaction conditions, the substrate scope was expanded to various allylbenzoates to further evaluate the catalytic activity of HG₂@HMPNs (Scheme 2). Whatever the electron-donating (R¹ = CH₃, CH₂CH₃, *t*-Bu) or electron-withdrawing substituent groups (R₁ = F, NO₂) that are attached to the phenyl ring of the allylbenzoates, HG₂@HMPNs affords good product yields (81–88%) comparable to those when using the homogeneous HG₂ catalyst (83–90%). The reduction in yield of less than 3% suggests that the characteristic morphology of HG₂@HMPNs with their hollow interior and mesoporous and swellable shell facilitates efficient mass transfer of reactants to the Ru catalytic sites, even under heterogeneous conditions. Unfortunately, HG₂@HMPNs promote the reactions of bulky allyl naphthalate and allylbenzoate (R₂ = Ph) with crotonaldehyde to afford the corresponding products in significantly lower yields. Compared with the homogeneous HG₂ catalyst, HG₂@HMPNs afford the corresponding products with yield reductions of 8% and 13%, respectively. The reason for this is attributed to limited mass transfer within the porous channels of HG₂@HMPNs, where bulky allylbenzoates bearing naphthyl and biphenyl moieties encounter steric hin-



Scheme 2 Olefin metathesis of various allylbenzoates with crotonaldehyde catalysed by $\text{HG}_2\text{@HMPNs}$ (Cat. A) and homogeneous HG_2 catalyst (Cat. B). Reaction conditions: allylbenzoates (1.0 mmol), crotonaldehyde (70.1 mg, 1.0 mmol), toluene (2 mL), $\text{HG}_2\text{@HMPNs}$ (108.0 mg, 5.0 mol% of HG_2 catalyst), 20 °C, 30 min.

drance from the pore walls, leading to limited access to interior Ru catalytic sites. To improve the reactivity of bulky allylbenzoates, the amount of cross-linking agent (DVB) used in the preparation of HMPNs was reduced by 20%. The obtained $\text{HG}_2\text{@HMPNs}$ with their enhanced swellability affords products at significantly improved yields of 84% and 81%, respectively, due to the larger pore sizes of HMPNs in organic solvent. Unfortunately, a further decrease, where the amount of DVB was reduced by 40% causes HMPNs to lose their well-defined spherical morphology. Moreover, in comparison with homogeneous catalysis, there is no change in the *E/Z* outcomes of products.

Following completion of the olefin metathesis of 2,4,6-trimethylbenzoate and crotonaldehyde, $\text{HG}_2\text{@HMPNs}$ can be easily recovered *via* centrifugation, washed with ethyl acetate, dried naturally, and reused directly in subsequent catalytic cycles. As shown in Fig. 3a, gram-scale heterogeneous olefin metatheses show no significant decrease in yield during eight cycles of using $\text{HG}_2\text{@HMPNs}$. The morphology, Ru content and porous structure of the 8th-reused $\text{HG}_2\text{@HMPNs}$ were characterized by SEM, ICP-OES and N_2 adsorption-desorption isotherms. It can be seen from the SEM image that the 8th-reused $\text{HG}_2\text{@HMPNs}$ maintain the well-defined spherical morphology observed in the freshly made $\text{HG}_2\text{@HMPNs}$ (Fig. 3b), indicating that $\text{HG}_2\text{@HMPNs}$ possess good mechanical stability.

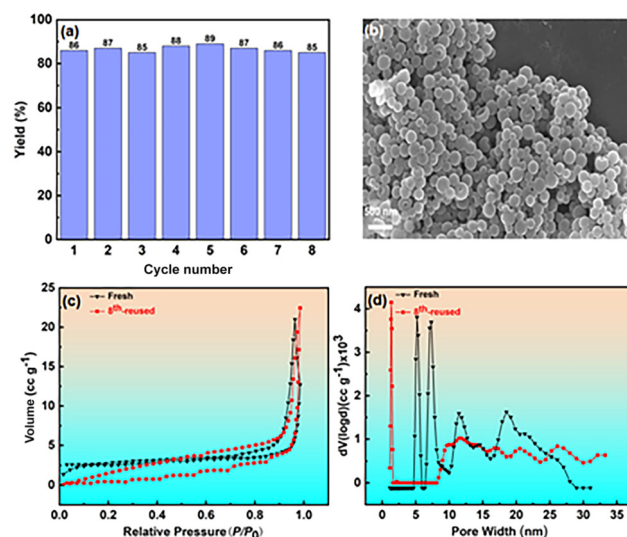


Fig. 3 (a) Yields of product following the reuse of $\text{HG}_2\text{@HMPNs}$ during the olefin metathesis of allylbenzoate and crotonaldehyde under the following conditions: 2,4,6-trimethylbenzoate (1.02 g, 5.0 mmol), crotonaldehyde (0.35 g, 5.0 mmol), toluene (10 mL), $\text{HG}_2\text{@HMPNs}$ (0.54 g, 5.0 mol% Ru), 20 °C, 30 min. (b) SEM image of the 8th-reused $\text{HG}_2\text{@HMPNs}$. (c) N_2 adsorption-desorption isotherms and (d) pore size distributions of the pristine and 8th-reused $\text{HG}_2\text{@HMPNs}$.

Furthermore, the Ru content in the 8th-reused $\text{HG}_2\text{@HMPNs}$, as determined by ICP-OES, was found to be 0.44 mmol g⁻¹, revealing that the covalently anchored HG_2 catalyst exhibits good chemical stability during repeated catalytic processes. Notably, the Ru concentration in the corresponding reaction mixtures remained in the range of 0.008–0.012‰ during the catalytic cycles, as measured by ICP-OES. Following purification of the reaction residue by column chromatography, no detectable ruthenium was found in the isolated pure products. Moreover, the N_2 adsorption-desorption isotherms reveal no obvious change in the total adsorbed volume of N_2 (Fig. 3c). In contrast, the pore size distribution of the 8th-reused $\text{HG}_2\text{@HMPNs}$ differs greatly in comparison with that of the pristine sample. The mesopores originally centered at 5.2 nm and 7.5 nm disappear, while new micropores centered at 1.3 nm have emerged, possibly resulting from the accumulation of reactants and/or products within these pores. Owing to the maintenance of the mesopores above 8 nm, the mass transfer of reactants is not significantly affected. Therefore, it is considered that the blockage of the mesopores by reactants and/or products and the negligible loss of anchored Ru catalyst are responsible for the small decreases in yield during the reuse of $\text{HG}_2\text{@HMPNs}$.

In this communication, the HG_2 catalyst is directly immobilized onto HMPNs *via* Friedel-Crafts alkylation, without prior molecular modification. This strategy avoids the previously reported multi-step molecular modification of the catalyst, effectively improving the utilization of the HG_2 catalyst. The as-fabricated HMPN-supported HG_2 catalyst possesses a hollow interior and a thin, mesopore-abundant shell, provid-

ing an architecture ideally suited to the fast mass transfer of reactants to facilitate access to Ru catalytic sites. In the heterogeneous olefin metathesis of allylbenzoates and crotonaldehyde, comparable yields to homogeneous counterparts and good reusability of the catalyst can be achieved. Overall, this direct immobilization of the HG₂ catalyst onto HMPNs *via* Friedel–Crafts alkylation provides a reference for the immobilization of other expensive HG catalysts, achieving the low-cost synthesis of fine chemicals.

Author contributions

Chuangchuang He: Investigation, visualization, methodology, formal analysis, validation, and writing – original draft; Jincheng Duan: Investigation; Yang Zhou: Investigation; Junling Cui: Investigation; Xuebing Ma: Conceptualization, funding acquisition, project administration, methodology, and writing – review & editing.

Conflicts of interest

There are no conflicts to declare.

Data availability

The data supporting this article have been included as part of the ESI.†

Acknowledgements

This work was financially supported by the National Natural Science Foundation of China (51973177).

References

- O. M. Ogbay, N. C. Warner, D. J. O'Leary and R. H. Grubbs, *Chem. Soc. Rev.*, 2018, **47**, 4510–4544.
- D. F. Sauer, J. Schiffels, T. Hayashi, U. Schwaneberg and J. Okuda, *Beilstein J. Org. Chem.*, 2018, **14**, 2861–2871.
- M. Jeschek, S. Panke and T. R. Ward, *Trends Biotechnol.*, 2018, **36**, 60–72.
- G. I. Peterson, S. Yang and T. L. Choi, *Acc. Chem. Res.*, 2019, **52**, 994–1005.
- T. Tiso, D. F. Sauer, K. Beckerle, C. C. Blesken, J. Okuda and L. M. Blank, *Catalysts*, 2020, **10**, 874.
- H. Yang, Z. Ma, T. Zhou, W. Zhang, J. Chao and Y. Qin, *ChemCatChem*, 2013, **5**, 2278–2287.
- M. Aşkun, K. Sagdic, F. Inci and B. Ö. Öztürk, *Catal. Sci. Technol.*, 2022, **12**, 6174–6183.
- Z. Tunalı, K. Sagdic, F. Inci and B. Ö. Öztürk, *React. Chem. Eng.*, 2022, **7**, 1617–1625.
- Q. Li, T. Zhou and H. Yang, *ACS Catal.*, 2015, **5**, 2225–2231.
- B. Ö. Öztürk, A. Hillik, B. N. Küçük and F. Inci, *Dalton Trans.*, 2025, **54**, 8658.
- M. Al-Hashimi, R. Tuba, H. S. Bazzi and R. H. Grubbs, *ChemCatChem*, 2015, **8**, 228–233.
- M. O. Lvanysya, S. V. Ryabukhin, D. M. Volochnyuk and S. V. Kolotilov, *Theor. Exp. Chem.*, 2020, **56**, 283–308.
- R. Duque, E. Öchsner, H. Clavier, F. Caijo, S. P. Nolan, M. Mauduit and D. J. C. Hamilton, *Green Chem.*, 2011, **13**, 1187–1195.
- M. Al-Hashimi, R. Tuba, H. S. Bazzi and R. H. Grubbs, *ChemCatChem*, 2015, **8**, 228–233.
- G. Liu and J. Wang, *Angew. Chem., Int. Ed.*, 2010, **49**, 4425–4429.
- Y. Duan, T. Wang, Q. Xie, X. Yu, W. Guo, S. Wu, D. Li, J. Wang and G. Liu, *Dalton Trans.*, 2017, **46**, 5986–5993.
- M. Matsugi and D. P. Curran, *J. Org. Chem.*, 2005, **70**, 1636–1642.
- D. Schoeps, K. Buhr, M. Dijkstra, K. Ebert and H. Plenio, *Chem. – Eur. J.*, 2009, **15**, 2960–2965.
- J. Pastva, K. Skowerski, S. J. Czarnocki, N. Žilková, J. Čejka, Z. Bastl and H. Balcar, *ACS Catal.*, 2014, **4**, 3227–3236.
- E. Borré, M. Rouen, I. Laurent, M. Magrez, F. Caijo, C. Crévisy, W. Solodenko, L. Toupet, R. Frankfurter, C. Vogt, A. Kirschning and M. Mauduit, *Chem. – Eur. J.*, 2012, **18**, 16369–16382.
- N. J. M. Pijnenburg, E. Tomás-Mendivil, K. E. Mayland, H. Kleijn, M. Lutz, A. L. Spek, G. van Koten and R. J. M. K. Gebbink, *Inorg. Chim. Acta*, 2014, **409**, 163–173.
- J. L. Cheong, D. Wong, S. G. Lee, J. Lim and S. S. Lee, *Chem. Commun.*, 2015, **51**, 1042–1045.
- H. Balcar, N. Žilková, M. Kubů, M. Polášek and J. Zedník, *Catal. Today*, 2018, **304**, 127–134.
- B. Werghi, E. Pump, M. Tretiakov, E. A. Hamad, A. Gurinov, P. Doggali, D. H. Anjum, L. Cavallo, A. Bendjeriou-Sedjerari and J. M. Basset, *Chem. Sci.*, 2018, **9**, 3531–3537.
- P. D. Nieres, V. A. Vaillard, J. Zelín, N. I. Neuman, A. F. Trasarti, C. R. Apesteguía and S. E. Vaillard, *ChemCatChem*, 2023, **15**, e202300010.
- J. Lim, S. S. Lee, S. N. Riduan and J. Y. Ying, *Adv. Synth. Catal.*, 2007, **349**, 1066–1076.
- J. Lim, S. S. Lee and J. Y. Ying, *Chem. Commun.*, 2010, **46**, 806–808.
- H. Yang, Z. Ma, Y. Wang, Y. Wang and L. Fang, *Chem. Commun.*, 2010, **46**, 8659–8661.
- D. P. Allen, M. M. Van Wingerden and R. H. Grubbs, *Org. Lett.*, 2009, **11**, 1261–1264.
- J. Cabrera, R. Padilla, M. Bru, R. Lindner, T. Kageyama, K. Wilckens, S. L. Balof, H. J. Schanz, R. Dehn, J. H. Teles, S. Deuerlein, K. Müller, F. Rominger and M. Limbach, *Chem. – Eur. J.*, 2012, **18**, 14717–14724.
- M. P. Conley, C. Copéret and C. Thieuleux, *ACS Catal.*, 2014, **4**, 1458–1469.
- C. del Pozo, A. Corma, M. Iglesias and F. Sánchez, *J. Catal.*, 2012, **291**, 110–116.

- 33 B. Marciniak, S. Rogalski, M. J. Potrzebowski and C. Pietraszuk, *ChemCatChem*, 2011, **3**, 904–910.
- 34 A. Monge-Marcet, R. Pleixats, X. Cattoën and M. W. C. Man, *J. Mol. Catal. A: Chem.*, 2012, **357**, 59–66.
- 35 A. M. Marcet, R. Pleixats, X. Cattoën and M. W. C. Man, *Tetrahedron*, 2013, **69**, 341–348.
- 36 H. Nasrallah, A. Pagnoux, D. Didier, C. Magnier, L. Toupet, R. Guillot, C. Crévisy, M. Mauduit and E. Schulz, *Eur. J. Org. Chem.*, 2014, 7781–7787.
- 37 H. Nasrallah, D. Dragoe, C. Magnier, C. Crévisy, M. Mauduit and E. Schulz, *ChemCatChem*, 2015, **7**, 2493–2500.
- 38 M. K. Samantaray, J. Alauzun, D. Gajan, S. Kavita, A. Mehdi, L. Veyre, M. Lelli, A. Lesage, L. Emsley, C. Copéret and C. Thieuleux, *J. Am. Chem. Soc.*, 2013, **135**, 3193–3199.
- 39 B. Van Berlo, K. Houthoofd, B. F. Sels and P. A. Jacobs, *Adv. Synth. Catal.*, 2008, **350**, 1949–1953.
- 40 H. Zhang, Y. Li, S. Shao, H. Wu and P. Wu, *J. Mol. Catal. A: Chem.*, 2013, **372**, 35–43.
- 41 S. W. Chen, J. H. Kim, C. E. Song and S. G. Lee, *Org. Lett.*, 2007, **9**, 3845–3848.
- 42 C. Hongfa, H.-L. Su, H. S. Bazzi and D. E. Bergbreiter, *Org. Lett.*, 2009, **11**, 665–667.
- 43 A. Kirschning, K. Mennecke, K. Grela and U. Kunz, *Synlett*, 2005, **19**, 2948–2952.
- 44 Q. Yao and Y. Zhang, *J. Am. Chem. Soc.*, 2004, **126**, 74–75.
- 45 C. Hobbs, Y. C. Yang, J. Ling, S. Nicola, H. L. Su, H. S. Bazzi and D. E. Bergbreiter, *Org. Lett.*, 2011, **13**, 3904–3907.
- 46 L. Xia, T. Peng, G. Wang, X. Wen, S. Zhang and L. Wang, *ChemistryOpen*, 2019, **8**, 45–48.
- 47 D. V. Espinosa, C. Vicent, M. Baya and J. A. Mata, *Catal. Sci. Technol.*, 2016, **6**, 8024–8035.
- 48 S. Lee, J. Y. Shin and S. g. Lee, *Chem. – Asian J.*, 2013, **8**, 1990–1993.
- 49 G. Liu, B. Wu, J. Zhang, X. Wang, M. Shao and J. Wang, *Inorg. Chem.*, 2009, **48**, 2383–2390.
- 50 S. Sabater, J. A. Mata and E. Peris, *ACS Catal.*, 2014, **4**, 2038–2047.
- 51 B. Ö. Öztürk, *Microporous Mesoporous Mater.*, 2018, **267**, 249–256.
- 52 S. W. Chen, Z. C. Zhang, M. Ma, C. M. Zhong and S. g. Lee, *Org. Lett.*, 2014, **16**, 4969–4971.
- 53 Y. H. Zhu, L. Kuijin, N. Huimin, C. Z. Li, L. P. Stubbs, C. F. Siong, T. Muihua and S. C. Peng, *Adv. Synth. Catal.*, 2009, **351**, 2650–2656.
- 54 C. C. He, J. P. Duan and X. B. Ma, *Mol. Catal.*, 2024, **567**, 114480.
- 55 J. N. Zhang and X. B. Ma, *Appl. Catal., A*, 2024, **675**, 119633.
- 56 M. Y. Xie, W. Y. Tian and X. B. Ma, *Appl. Catal., A*, 2024, **684**, 119905.
- 57 J. Liu, H. Zhu, J. N. Zhang, W. Y. Tian and X. B. Ma, *J. Catal.*, 2023, **425**, 322–332.
- 58 W. Y. Tian, Y. Y. Luo, S. W. Zhu, Y. Zhou, C. C. He and X. B. Ma, *Dalton Trans.*, 2025, **54**, 8055–8060.
- 59 J. N. Zhang, S. Li, J. Liu and X. B. Ma, *Appl. Catal., A*, 2023, **649**, 118976.
- 60 S. Li, J. N. Zhang, S. Q. Chen and X. B. Ma, *J. Catal.*, 2022, **416**, 139–148.
- 61 G. X. Xie, S. Wei, L. Zhang and X. B. Ma, *Ind. Eng. Chem. Res.*, 2019, **58**, 2812–2823.
- 62 R. L. Pederson, I. M. Fellows, T. A. Ung, H. Ishihara and S. P. Hajela, *Adv. Synth. Catal.*, 2002, **344**, 728–735.